

行政院國家科學委員會專題研究計畫 成果報告

寬頻合作式無線多輸出入通訊系統--子計畫二：合作式多 輸出入下行考慮同步不確定之傳收器設計(2/2) 研究成果報告(完整版)

計畫類別：整合型
計畫編號：NSC 99-2219-E-009-009-
執行期間：99年08月01日至100年07月31日
執行單位：國立交通大學電子工程學系及電子研究所

計畫主持人：桑梓賢

計畫參與人員：碩士班研究生-兼任助理人員：呂宗達
碩士班研究生-兼任助理人員：連哲聖
碩士班研究生-兼任助理人員：李俊育
碩士班研究生-兼任助理人員：蔡耀賢
碩士班研究生-兼任助理人員：林建志
博士班研究生-兼任助理人員：林欣德

報告附件：出席國際會議研究心得報告及發表論文

處理方式：本計畫涉及專利或其他智慧財產權，2年後可公開查詢

中華民國 100 年 08 月 31 日

行政院國家科學委員會補助專題研究計畫

成果報告
 期中進度報告

寬頻合作式無線多輸出入通訊系統—子計畫二：合作式多輸出入下行考慮同步不確定之傳收器設計(2/2)

計畫類別： 個別型計畫 整合型計畫

計畫編號：NSC 99 - 2219 - E - 009 - 009

執行期間：99 年 8 月 1 日至 100 年 7 月 31 日

執行機構及系所：國立交通大學電子工程學系(所)

計畫主持人：桑梓賢

共同主持人：

計畫參與人員：林欣德、呂宗達、林哲聖、李俊育、蔡耀賢

成果報告類型(依經費核定清單規定繳交)： 精簡報告 完整報告

本計畫除繳交成果報告外，另須繳交以下出國心得報告：

- 赴國外出差或研習心得報告
- 赴大陸地區出差或研習心得報告
- 出席國際學術會議心得報告
- 國際合作研究計畫國外研究報告

處理方式：除列管計畫及下列情形者外，得立即公開查詢

涉及專利或其他智慧財產權， 一年 二年後可公開查詢

中 華 民 國 100 年 8 月 30 日

摘要

本計畫所設定的研究目標為：解決寬頻合作式無線多輸出入通訊系統在用戶端高速移動下，因通道衰落及同步誤差所造成的系統效能損失。高速移動環境所造成的通道衰落及載波間干擾問題，一直是無線通訊的核心問題，我們從實用角度出發，重新檢視現有方法的侷限，並提出新的解決方案。合作式系統因 4G 標準開始討論協作式多點傳輸 (CoMP) 而有了新的意義，但如何解決多點同步問題也浮上檯面。互相合作形成陣列的天線分散在極為不同的傳輸環境中，因而無法像傳統處於同一地點的傳送天線陣列達成載波頻率及符元時間的完全同步。我們經由兩個面向提出同步問題的解決方案。首先我們從設計接收機著手，我們考慮廣泛使用的阿拉木提多輸出入系統，為其設計一套對同步誤差具有超強容忍力的接收機，數值模擬結果表明它運用於單載波系統可抵抗極大的載波頻率誤差，運用於多載波系統則可抵抗極大的符元時間誤差。另外，我們也從編碼設計的角度解決同步問題。在這裡，我們不將同步誤差視做必須避免的問題，反而視為多集性增益的可能來源。經由為合作式多輸出入通訊設計一種位元交錯編碼調變方式，我們發現，當同步誤差存在時，多集性增益也大幅增加。

關鍵詞：合作式通訊、協作式多點傳輸、正交分頻多工、載波間干擾、同步、阿拉木提、位元交錯編碼調變

Abstract

The goal set in this project is to solve issues caused by fading channels and synchronization errors arise from deploying broadband cooperative Multiple-Input Multiple-Output (MIMO) systems with highly mobile users. Performance degradation caused by fading channels and inter-carrier interference has always been a core issue for mobile communications. We consider these problems from the angle of practical deployment and point out limitations of various existing advanced methods. We also provide a good and practical solution. Cooperative MIMO obtains new meanings since the 4G standard meetings began discussing Coordinated Multi-Point (CoMP) transmission. This also leads to the urgent needs to solve unique challenges of synchronization. The synchronization issues have unique characteristics due to the fact that cooperating transmitters may be distributed physically and thus may be situated in widely different transmission environments, contrasting to co-located transmitters with which the carrier frequencies and symbol clocks can be synchronized perfectly. In this project we aim to addressing synchronization errors in cooperative MIMO systems from two perspectives. The first is to design a receiver which is extremely tolerant with synchronization errors when used in combination with common Alamouti schemes. Simulation results show that the receiver can retain the diversity order even when large carrier frequency offsets exist in single-carrier systems and large symbol timing errors in multi-carrier systems. The second perspective is to solve the problem via code design. Instead of viewing synchronization errors as impairments, we treat them as potential sources of diversity gain. A Bit-Interleaved Coded Modulation (BICM) scheme is eventually developed for cooperative scenarios in which the diversity order can be dramatically increased when synchronization errors exist.

Key words: cooperative communications、CoMP、OFDM、inter-carrier interference、synchronization、Alamouti、BICM

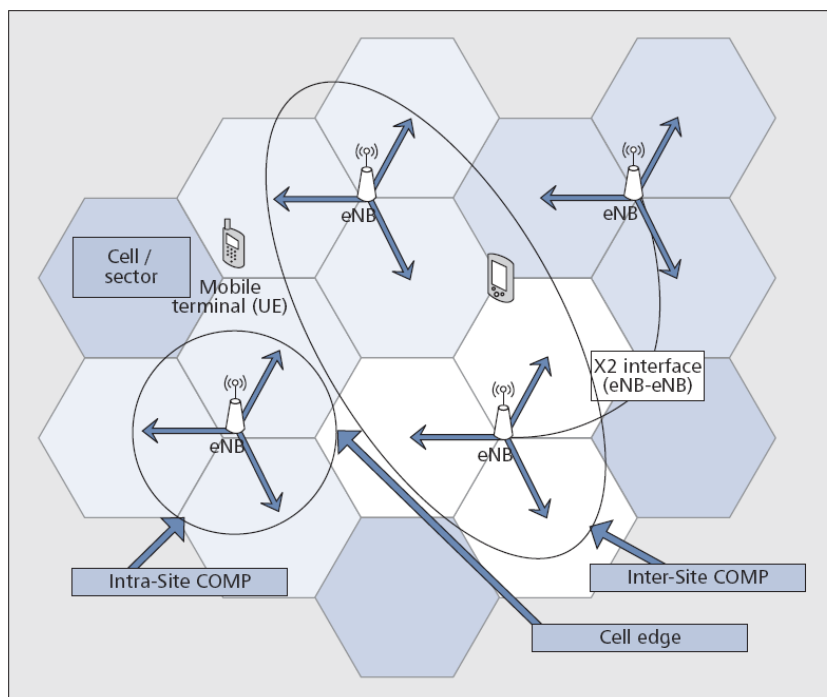
目錄

1. 前言	4
2. ICI Cancellation in OFDM Systems over Time Varying Channels.....	6
2.1 ICI Models	7
2.2 ICI Indicator.....	8
2.3 Per-subcarrier Adaptive ICI Cancellation Framework.....	10
2.4 Computational Complexity	13
3. Multiple Carrier Frequency Offsets in Cooperative Communications	14
3.1 System Model	15
3.2 Multiple CFOs Mitigation.....	17
3.3 Time-Frequency Duality and Single-Carrier Systems	19
3.4 Simulation Results	20
3. BICM-OFDM to Combat Multiple Synchronous Errors	22
3.1 System Model	22
3.2 The Receiver Algorithm.....	24
3.3 Simulation Results and Discussion.....	26
4. 結果與討論	28
5. 計劃成果自評	28
6. 參考文獻	29

1. 前言

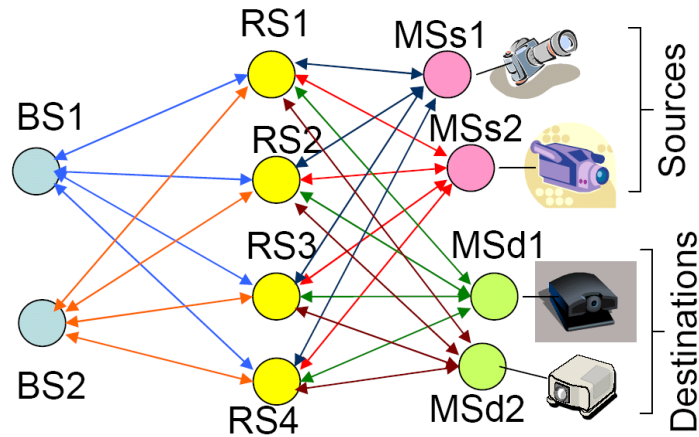
在第四代無線通訊系統中, 3GPP LTE (3rd Generation Partnership Project Long Term Evolution, 第三代合作夥伴計劃長期演進技術) 以傳輸距離長、傳輸速率高、佈建快、成本低等特性, 已和 WiMAX 成為最被看好的無線寬頻技術。LTE 的標準主要部分 Release 8 已於 2009 年完成[1]。參考各國際大廠日前介紹參與制定行動 LTE-advanced 和 WiMAX[2]規格的近況, 往後發展計畫要能在時速 350 Km/hr 的如此快速移動狀態下的傳輸速率可達 100 Mb/s, 在固定使用無線數據傳輸速率時可達 1Gb/s。

為了達到如此高的傳輸速率以及保持在高速移動狀態時訊號的可靠度, 必須採用 MIMO (多根傳輸天線-多根接收天線) 技術。而合作式(cooperative)或分散式(distributed)的 MIMO 技術更開始廣受標準組織的青睞。例如, LTE-advanced 開始討論協作式多點傳輸 Coordinated Multi-Point (CoMP) transmission 用以改善細胞邊緣的訊號條件及胞內傳輸速率的提升, 其工作原理示意圖如下所示。而 IEEE 802.16e 中規範了一個稱為「協力空間多工(collaborative spatial multiplexing)」的選項(optional)技術, 可以讓兩個用戶台協力進行上行傳輸, 但兩個用戶台需要知道彼此的上傳資料。IEEE 802.16j[3]所規範的是中繼站(relay station, RS)技術, 規範了中繼站群組(RS grouping)及合作中繼(cooperative relaying), 可以透過兩個或更多個中繼站來共同向同一用戶台傳送同樣的訊號。IMT-Advanced 可能也都會將協作式多點傳輸及中繼站視為整個系統的重要組件, 自始就納入標準規範。這些標準制定活動表明廣義上的合作式(cooperative) MIMO 會是熱門的無線通訊技術之一。



圖一、協作式多點傳輸 Coordinated Multi-Point (CoMP) transmission 示意圖[4]。

本子計畫基於總計畫提出的之合作式無線多輸出入通訊系統(請見下圖), 結合 4G 標準中實體層的下行部分(downlink)所採用的 OFDMA (Orthogonal Frequency Division Multiple Access, 正交分頻多工進接), 研究高速移動環境所造成的通道衰落及載波間干擾問題, 以及有多重同步誤差的情況下, 通道估測、接收機設計等下行相關議題, 以下就此一新技術趨勢之可能優點及待解決的下行訊號處理挑戰做一綜述。



圖二、參考系統架構示意圖, 其中 BS = base station, RS = relay station, MS = mobile station。

正交分頻多工(OFDM)系統以其高度頻譜效能著稱, 且是 4G 標準的傳輸技術不二人選, 在標準要求的高速移動狀況下, 通道將會受到強烈的多普勒效應(Doppler spreading), 同時也會有嚴重的衰落(fading), 正交分頻多工訊號會面臨一個很嚴重的問題, 即載波間干擾(inter-carrier interference, ICI), 文獻中已有許多減輕 ICI 的技術[5]-[16], 某些甚至有一流效能表現, 然而各種實際問題限制了它們的應用, 具成本效益與良好表現的方法仍為業界急需, 我們從實用角度出發, 重新檢視現有方法的侷限, 並提出新的解決方案。

合作式 MIMO 由於各基地台/中繼站參數以及與行動台間的通道狀況並不相同且時常改變, 因而帶來幾點可能的優勢[18]-[22]: 第一、更大的範圍延伸(range extension)。第二、解決因通道的鴿洞效應(pigeon hole effect)而導致的多集增益(diversity gain)的損失。第三、更彈性地使用頻帶達成吞吐量強化(throughput enhancement)。我們認為若更有效的利用不同使用者間的共同資訊(User Diversity)可進一步增進系統效能。

由於下行合作式多輸出入系統的特性, 有三項獨特的訊號處理議題亟需解決: 1. 因高速移動及多個基地台/中繼站各不相同的傳輸參數和都卜勒狀況而產生嚴重的訊號品質下降。2. 各基地台/中繼站對同一移動台而言有不同的最佳符元時間(symbol timing)以及載波頻率偏移(multiple carrier frequency offsets), 因而有同步的不確定性。3. 合作式 MIMO 系統的通道狀態資訊(CSI, Channel State Information)估測通常較點對點 MIMO 系統更為複雜, 因而簡單且有效的通道估測, 也是研究熱點。

本計畫針對同步誤差以及高速移動下的傳輸參數不確定性, 經由兩個面向提出解決方案。首先我們從設計接收機著手, 我們考慮廣泛使用的 Alamouti 多輸出入系統[23], 為其設計一套對同步誤差具有超強容忍力的接收機, 數值模擬結果表明它運用於單載波系統可

抵抗極大的載波頻率誤差，運用於多載波系統則可抵抗極大的符元時間誤差。另外、我們也從編碼設計的角度解決同步問題。在這裡，我們不將同步誤差視做必須避免的問題，反而視為多集性增益的可能來源。經由為合作式多輸出入通訊設計一種位元交錯編碼調變 (BICM) 方式[24]，我們發現、當同步誤差存在時、多集性增益竟大幅增加，我們也對此結果做了一些理論分析。至此、在 Alamouti 編碼以及 BICM 的情況下之同步問題，已獲得初步解決，唯目前開發的接收機演算法仍具高複雜度，降低複雜度也是我們努力的方向。

以下關於技術部分的章節，由於行文方便性的考量，將以英文撰寫，對讀者造成的任何不便，作者深表歉意。

2. ICI Cancellation in OFDM Systems over Time Varying

Channels

First, we address the most common anomaly that faces typical mobile devices, especially those devices that employ the current modulation technique of choice – OFDM. In time-varying (TV) channels, the channel frequency response (CFR) matrix of OFDM systems is no longer diagonal and the off-diagonal terms contribute to ICI. ICI can cause serious performance degradation in OFDM systems and many ICI cancellation techniques have been proposed over the years to deal with the imperfect CFR matrix; see [5]-[16] and references therein. In [5], [7], [8], [12], [15], frequency-domain zero-forcing (ZF) or minimum mean square error (MMSE) ICI equalizers are proposed, while time-domain equalizers are investigated in [6]. For these methods, the major computational cost comes from matrix inversion. So far the means to reduce the cost is imposing the ICI matrix to a banded structure in which all but few elements on selected diagonals are set to zero [5]. With the banded structure, matrix inversions of smaller sizes are used to calculate coefficients of MMSE or ZF ICI equalizers. A rule of thumbs in [9][12] is to choose the bandwidth parameter Q is $Q \geq \lceil f_D/\Delta f \rceil + 1$, where f_D is the maximum Doppler frequency and Δf denotes the subcarrier spacing. However, the BER performance can degrade severely when Q is not large enough.

Other advanced techniques such as nonlinear ICI equalizers offer superb performance, but they may have limited implementation readiness due to either higher computational cost or limitations specified by standards. Popular wireless broadband access technologies such as WiMAX (IEEE 802.16e) and LTE both choose orthogonal frequency division multiple access (OFDMA) as the downlink transmission scheme. This will cause problems for decision feedback or iterative equalizers, such as those in [7] and [9]; they may not be suitable for OFDMA due to the need to know CFR information or data on other users' or un-occupied subcarriers. Another

technique, the turbo ICI equalizer [13][14], requires CFR information, the feedback from the channel decoder, and has longer processing latency due to its iterative nature. Some techniques that utilize time-domain windowing [9][10] can greatly extend the supported Doppler spread range but the white noise will be colored and the receiver has to handle it to avoid performance degradation [17]. The MAP and MLSE equalizers [16] offer the best performance yet the cost is still too high. Methods based on basis expansion model [10][16] also need to consider issues of channel estimation and model fitting.

In short, to develop a simple ICI equalizer with adequate performance still means much practical significance to the communication industry. In this paper, we focus on improving the inner receiver and developing low-complexity methods that can provide decent performance for standards such as WiMAX or LTE. We start with a popular model of linearly time-varying channel is reviewed and some observations are noticed as the inspiration of our per-subcarrier approach. We propose a simple ICI indicator is proposed to show the relative severity of ICI on each individual subcarrier. Its statistical properties, in particular the probability density function (PDF), are investigated to lay a theoretical foundation for adapting the ICI equalizer according to the ICI indicator and estimating the possible saving in computational complexity. Based on the ICI indicator, a per-subcarrier adaptive framework which can work with most existing ICI cancellation methods, especially linear ICI equalizers, is proposed to further reduce computational complexity while maintaining performance. Several examples demonstrate how the framework operates. Especially, a novel low-complexity perturbation-based ICI equalizer is developed with the emphasis on implementation readiness and adequate performance. Simulations are provided and savings in computational cost are calculated to show the effectiveness of our approach.

2.1 ICI Models

Consider the baseband equivalent OFDM system model with N subcarriers, the length of one transmitted OFDM symbol is $N_S = N + N_{CP}$ in which N_{CP} is the length of the cyclic prefix. The received signal on the i -th subcarrier is:

$$R_i = \sum_{m=0}^{N-1} S_m H_{i,m} + Z_i, \quad i = 0, 1, \dots, N-1$$

where S_m is the data symbol on the m -th subcarrier, $H_{i,m}$ represents the Channel Frequency Response (CFR), and Z_i is white Gaussian noise. ICI on the i -th subcarrier caused by the signal on the m -th transmit subcarrier comes through the ICI channel $H_{i,m}$. We organize $H_{i,m}$ into a matrix and that is the ICI channel matrix \mathbf{H} . Thus we can compactly represent the ICI signal model in the matrix form:

$$\mathbf{r} = \mathbf{H}\mathbf{s} + \mathbf{z} = \mathbf{H}_{avg}\mathbf{s} + \mathbf{G}\Delta\mathbf{s} + \mathbf{z}$$

where \mathbf{H}_{avg} is the diagonal averaged channel matrix part which is not affected by the Doppler spread and Δ is a diagonal channel matrix variation part and \mathbf{G} is a fixed ICI channel gain matrix which together with Δ reflect the effect of Doppler spread.

The ICI model in provides more insights when it is examined at the subcarrier-level granularity. For example, the magnitude of a 32×32 CFR matrix and cross-sections at three different subcarriers are shown in Fig. 3. The first thing to notice is that there is no uniform band structure in the CFR matrix, since each subcarrier faces very different ICI situations. This observation gives us an idea of adapting the ICI-cancellation method according to the ICI situation on each sub-carrier. Once this is done, we expect that the computational cost of ICI cancellation can be dramatically decreased since most of the sub-carrier, even at very high speed, do not really need extensive ICI treatment. As can be seen from the next sub-section, this observation is verified by studying the statistical properties of a certain ‘‘ICI indicator’’.

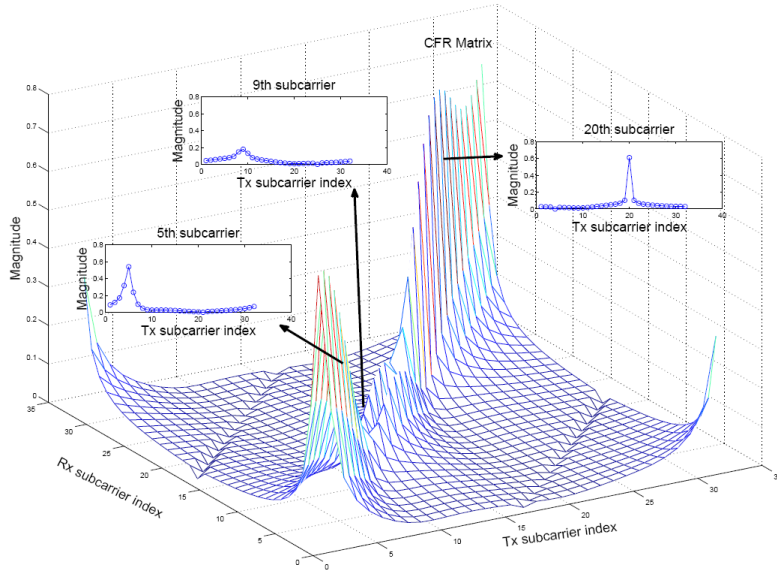


Fig. 3. The magnitude of a typical ICI channel matrix for a highly mobile user terminal

2.2 ICI Indicator

From Fig. 3, we see that the ICI situations at each sub-carrier are quite different. Therefore, we would like to devise a measurement which can reflect the different ICI situation at each sub-carrier. It is found that the ratio Δ_k/H_k (k is the sub-carrier index) can do the job. Given a value of $|\Delta_k/H_k|$, the corresponding signal-to-interference ratio (SIR) can be easily calculated. In Fig. 3, the 20-th subcarrier, with a small $|\Delta_k/H_k|$ ($|\Delta_k/H_k| < -5$ dB, roughly corresponds to SIR $>$

22 dB), is affected by insignificant amount of ICI and requires no ICI cancellation. When the signal experiences moderate fading, like on the 5-th subcarrier, $|\Delta_k/H_k|$ becomes higher (between -5 and 0 dB, corresponding to SIR from 22 to 12 dB), and a small truncated CFR matrix, say a 3×3 matrix, might be needed for adequate ICI cancellation. If deep fading occurs, as on the 9-th subcarrier, $|\Delta_k/H_k|$ becomes significant ($|\Delta_k/H_k| > 0$ dB corresponds to SIR < 12 dB), and a larger CFR sub-matrix will be needed for ICI cancellation. The term $|\Delta_k/H_k|$ seems able to reflect the ICI situation on each subcarrier.

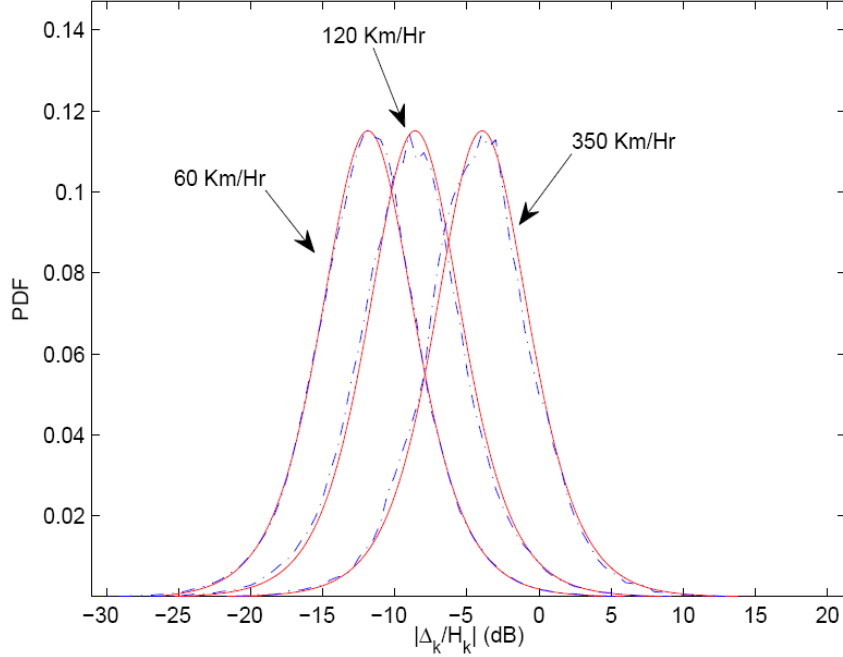


Fig. 4. Probability density functions (solid) and histograms (dash-dotted) of the ICI indicator for vehicle speed at 60, 120, and 350 km/h.

To better utilize $|\Delta_k/H_k|$ as the ICI indicator, its statistical properties need to be investigated. Assume Rayleigh fading channels, Δ_k and H_k can be approximated by two independent complex Gaussian random variables (RVs), and their absolute values follow the Rayleigh distribution. We found that the PDF of $|\Delta_k/H_k|$ can be found by calculating the convolution of two log-Rayleigh PDFs. Simulation is conducted to verify the derived PDF, using WiMAX standard with 10 MHz bandwidth, 2.5 GHz central carrier frequency, 1024 subcarriers, and the ITU Vehicular-A channel model. Fig. 4 shows the theoretical PDF and the histogram $10\log_{10}(|\Delta_k/H_k|)$ for various vehicle speeds, and they coincide closely. Recall that larger $|\Delta_k/H_k|$ means higher ICI level, it can be seen that as vehicle speed gets higher, more subcarriers experience severe ICI; yet even at 350 km/h, there are still 85% of subcarriers on which $|\Delta_k/H_k| < 0$ dB and simple ICI equalizers may be good enough. It is worth noting that the distribution of $10\log_{10}(|\Delta_k/H_k|)$ does not depend on the channel's power delay profile (PDP) since no assumption about the PDP needs to be made in the derivation. This is also confirmed through simulations with other channel models. Table I lists

the percentages of the ICI indicator in four ranges (≤ -5 dB, $-5 \sim -3$ dB, $-3 \sim 0$ dB, and ≥ 0 dB) against various vehicle speeds. The table can also be used in evaluating the benefit of reducing complexity by adapting ICI cancellers according to the ICI indicator.

TABLE I
ICI indicator, distribution under different vehicle speed

$ \Delta_k/H_k $	≤ -5 dB	$-5 \sim -3$ dB	$-3 \sim 0$ dB	≥ 0 dB
60 km/h	90.4%	4.0%	2.2%	3.5%
120 km/h	79.7%	9.6%	5.9%	4.9%
250 km/h	55.4%	18.9%	15.9%	9.7%
350 km/h	38.9%	21.8%	24.9%	15.4%

2.3 Per-subcarrier Adaptive ICI Cancellation Framework

We have learned that the ICI situation is quite different for each sub-carrier. So an intuitive way to treat ICI is to adaptively adjust your method from sub-carrier to sub-carrier.

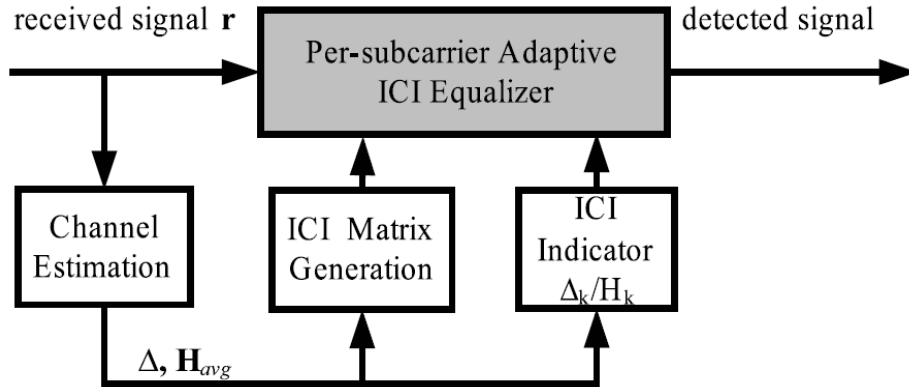


Fig. 5. Per-subcarrier adaptive ICI cancellation framework

Fig. 5 shows our proposed receiver architecture utilizing the ICI indicator. The per-subcarrier adaptive ICI equalizer adjusts its setting according to $|\Delta_k/H_k|$. The overall computational complexity can be greatly reduced with little performance degradation. The concept is simple and intuitive, yet has not been seen in the existing literature. In addition, it works well with popular wireless access technologies such as WiMAX and LTE based on OFDMA. Not only can it be exploited in signal detection but also used for channel estimation, in

which only the averaged CFR (H_k) needs to be estimated and (Δ_k) is simply the difference between H_k of adjacent OFDM symbols. Next, two examples are shown on how the framework incorporates conventional ICI equalizers.

First, consider linear equalizers. In a linear “block” ICI equalizer, usually a bandwidth parameter Q is chosen and only the lower and upper Q diagonal in the ICI channel matrix are considered and the whole banded ICI channel matrix is inverted to generate equalized signals. The parameter Q is selected according to the channel condition, but the value, once chosen, is fixed for all sub-carriers.

In a linear “serial” ICI equalizer, a smaller $(2Q+1)\times(2Q+1)$ matrix is inverted for each sub-carrier, since the whole ICI channel matrix is not inverted, the computational cost is dramatically reduced. But, again, the value of Q , once chosen, remains the same for all sub-carriers.

In our approach, however, instead of a fixed Q for every subcarrier, it is chosen according to $|\Delta_k/H_k|$. In this way, much computation cost is saved without hurting performance. Note that block and serial ZF equalizers can be easily obtained.

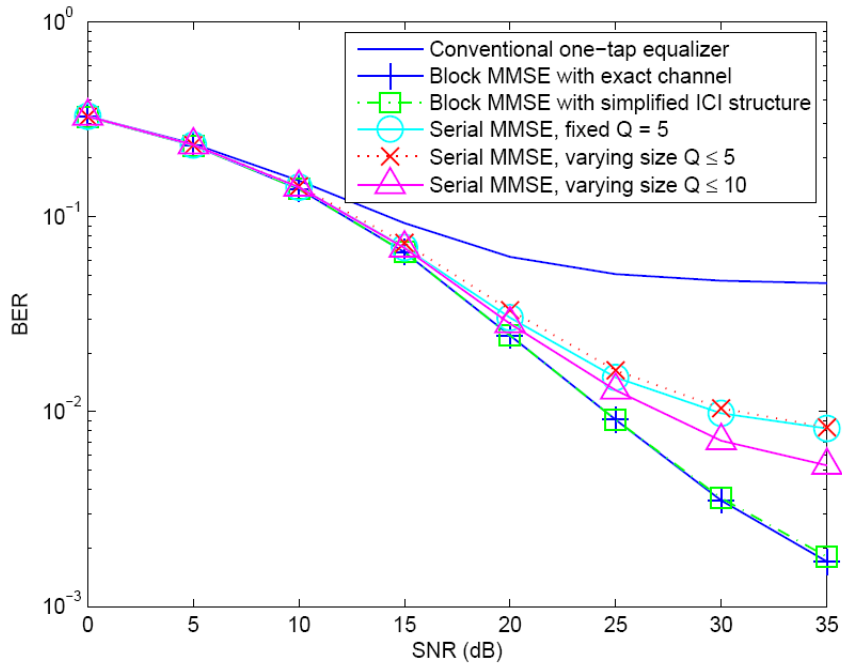


Fig. 6. BER performance comparisons for linear ICI equalizers under 1024-point FFT, 64-QAM, and ITU Vehicular-A channel model at 350 km/h.

Fig. 6 shows results with un-coded systems. So, what happens when channel coding is added? It is worth noting that our proposed methods far exceed the performance requirements of say, the WiMAX standard when mandatory channel coding is used. For example, our per-subcarrier adaptive ZF perturbation method achieves 10% packet error rate at 16 dB SNR at

350 km/h, while the standard requires only 60 km/h. Follow the same simulation set-up in Section III with $N_A = 864$ active subcarriers in the 1024-point FFT mode, BER comparisons of different ICI equalizers are shown in Fig. 6. The block MMSE ICI equalizer needs to invert a 864×864 matrix, either with the exact CFR matrix or a simplified approximation. The serial MMSE ICI equalizer inverts a local small CFR sub-matrix for each subcarrier to achieve lower complexity. The matrix size is set by Q which conventionally is fixed for all subcarriers. Our per-subcarrier adaptive ICI equalizer adjusts Q according to the ICI indicator. In our simulation, Q is chosen from the four settings ($Q = 0, 1, 3, \text{ and } 5$) corresponding to the four ranges (≤ -5 dB, $-5 \sim -3$ dB, $-3 \sim 0$ dB, and ≥ 0 dB) of $|\Delta_k/H_k|$. As shown in Fig. 4, our adaptive serial MMSE ICI equalizer with $Q \leq 5$ achieves, with significantly lower complexity, the same BER as the conventional one with fixed $Q = 5$. Overall, around 86% and 78% of computation can be saved when the velocity is kept under 250 and 350 km/h. On the other hand, with a comparable complexity, our per-subcarrier approach can afford a larger upper limit on Q , say using $Q = 10$ for the last range, and achieve much improved performance.

Next we consider how to incorporate with the Maximum APosterior (MAP) equalizer. The MAP equalizer offers the optimal performance yet is very costly. In our approach, reduction in computational complexity is achieved by reducing the size of trellis at most subcarriers. Note that the computational complexity of MAP equalizer grows exponentially which is in proportion to the number of states $M_{(2Q+1)}$ at each trellis stage if M -ary modulation is adopted. It is obvious that our per-subcarrier approach adjusting Q adaptively will dramatically reduce the complexity, especially for the high order modulation.

The MAP equalizer, even with a variable-size trellis, is still very costly to implement. In Fig. 7, a simpler simulation setting with QPSK is used to save simulation time. The result verifies that adjusting trellis size does not hurt the performance even when the speed hits 500 km/h. The MAP ICI equalizer with variable-size trellis attains the same BER performance as that of the MAP ICI equalizer with fixed-size trellis (in fact, their BER curves overlap each other), yet the computational cost is significantly reduced. Further reduction of complexity is possible if some techniques reported in recent literatures can be incorporated in the future. It is interesting that for the case when $Q \leq 3$, the MAP ICI equalizer performs better than the block MMSE ICI equalizer. It is due to the extra gain provided by combining signals along different ICI paths constructively.

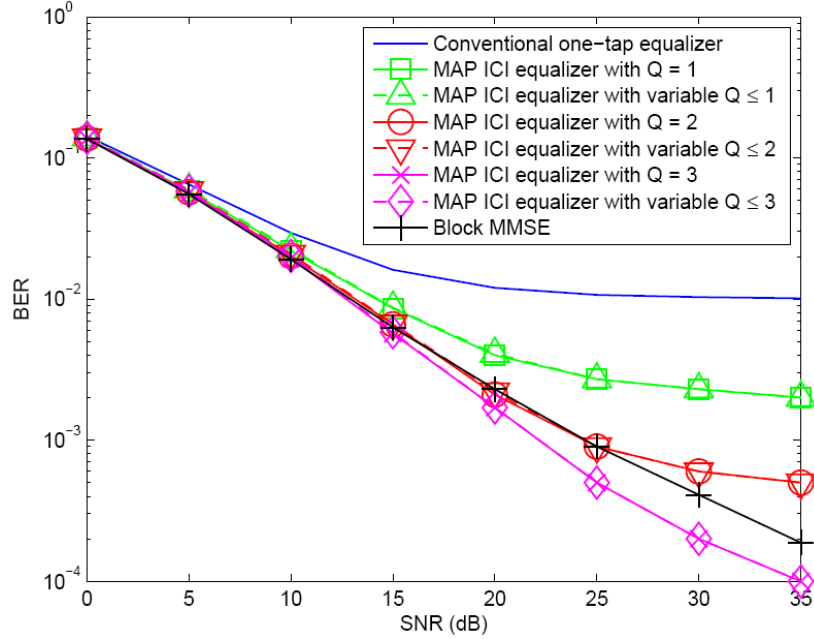


Fig. 7. BER performance comparisons for MAP ICI equalizers under 1024-point FFT, QPSK and ITU Vehicular-A channel model at 500 km/h. Note that the BER curves of MAP ICI equalizers (solid) overlap that of MAP ICI equalizers with variable size (dash).

2.4 Computational Complexity

We discuss the computational complexity measured in complex floating point operations (flops). The reduction of computational cost in conventional linear ICI equalizers by being incorporated into our per-subcarrier adaptive framework is demonstrated. The low computational complexity of the novel perturbation-based ICI equalizer is also clearly laid out. The complexity of the ICI equalizers comes from calculating equalizer coefficients and applying equalizers. Both aspects benefits from our approach. Only the complexity of calculating equalizer coefficients is considered here for simplicity because it accounts for the majority of the computational complexity. With the same simulation setting, the computational complexity of the block equalizer is approximately $2N_A^3/3 \approx 4 \times 108$ flops and that of the banded serial equalizer is approximately $N_A \times 2(2Q+1)3/3 \approx 7.5 \times 105$ flops with $Q = 5$.

Consider the per-subcarrier adaptive framework incorporating serial MMSE ICI equalizers. At the vehicle speed of 350 km/h, according to Table I, 38.9% of subcarriers use one-tap FEQ requiring $0.389 N_A$ flops, 21.8% of subcarriers use 3×3 matrix inversion requiring approximately $0.218 N_A \times 33 \times 2/3$ flops, 24.9% of subcarriers use 7×7 matrix inversion requiring $0.249 N_A \times 73 \times 2/3$ flops, and 15.4% of subcarriers use 11×11 matrix inversion requiring $0.154 N_A \times 113 \times 2/3$ flops. Overall, the complexity of the per-subcarrier adaptive serial ICI equalizer is approximately 1.6×105 flops at 350 km/h and the number for 250 km/h is

105, which are 22.2% and 14.2% of the number of flops of the conventional banded serial equalizer. In short, for any methods adopting banded approximation, the per-subcarrier adaptive framework can help further computational complexity reduction.

In summary, an informative indicator of ICI level and a per-subcarrier processing framework is proposed; they can work with many existing ICI cancellation methods to reduce the computational complexity and maintain the performance simultaneously. Theoretical analysis and simulations verify our claims. High flexibility is achieved for trade-off between performance and implementation cost.

3. Multiple Carrier Frequency Offsets in Cooperative

Communications

In this section, we address the first perspective of combating synchronization errors with the design of error-tolerant receivers. Notice that we situate our study in the context of utilizing space-time coding, especially Alamouti's space time block code (STBC) in the distributed (virtual) MIMO scenarios, due to its effectiveness of obtaining diversity gain as well as its low complexity.

As already mentioned, in distributed MIMO systems, each transmitter may have different local oscillators and may not be either frequency or time synchronized, i.e., there exist multiple symbol timing offsets (STOs) and multiple carrier frequency offsets (CFOs) [25]-[30]. It is well known that OFDM systems are sensitive to frequency offsets, and the performance can degrade significantly because of the inter-carrier interference (ICI) due to MCFOs. The resulting superposition of all cooperating nodes' signal causes standard CFO compensation techniques fail at the receiver. To deal with this problem, various mitigation techniques have been proposed in the literature[25]-[30].

Conventional equalizers can be used to combat multiple CFOs. A time domain equalizer, which aims to maximizing signal to interference and noise ratio (SINR) is proposed for space frequency coded system [25]. A simple method to convert the matrix inversion to a series of small inversions of its diagonal sub-blocks to reduce the calculation complexity is studied in [26]. In [27], several detection and complexity reducing techniques are compared. An ICI-self cancellation scheme at the price of lowering transmission rate is proposed in [28]. A special two branches receiver architecture is proposed in [29]. Based on the iterative inter-carrier interference (ICI) cancellation, a two-step cancellation procedure is developed in [30]. Iterative interference cancellation is yet another popular technique [31]. However, the performance of these techniques

degrades significantly as the magnitudes of MCFOs exceed a mild range.

In this section, synchronization for SFBC-OFDM is studied in the context of cooperative communications with synchronous errors. OFDM is robust to timing errors with a cyclic prefix insertion, so we focus on multiple CFOs. The separate synchronizing architecture in [29] is adopted, but a new SFBC demodulation technique based on [30] is used to increase the resulting SINR. In addition, iterative interference cancellation and a maximum-ratio-combining-like technique is also incorporated to further enhance the performance. The new receiver is computationally efficient and has a superior tolerance range of multiple CFOs and may be suitable for applications in asynchronous cooperative OFDM systems. We also demonstrate, through the time-frequency duality, that our procedure can be applied to combating symbol timing errors in single-carrier systems which is sensitive to this type of synchronization errors.

3.1 System Model

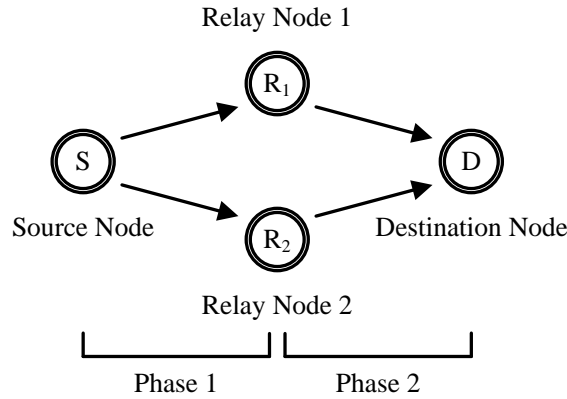


Fig. 8. A typical cooperative communication scenario

Consider a simplified cooperative transmission scheme with one source node, one destination node, and two relay nodes, as shown in Fig. 8. Each node has only one antenna. The decode-and-forward (DF) protocol is adopted [32]. In the first phase, the source node broadcasts the information sequence to the relay nodes. Without loss of generality, we assume that all relay nodes have correctly decoded the information sequence. In the second phase, all relay nodes remap the information sequence and cooperatively transmit it to the destination node.

Assume that a SFBC-OFDM based cooperative system is employed at the relay nodes. All the information sequences use the same signal constellation Γ , such as M-QAM or M-PSK, which can be denoted as $\mathbf{X} = [X_0, X_1, \dots, X_{Q-1}]^T$. The SFBC-OFDM modulates the symbol on two adjacent sub-carriers:

$$\begin{array}{c} \text{R e l a y 1} \\ \text{R e} \end{array} \quad \begin{array}{c} f_k \\ f_{k+1} \end{array} \quad \begin{bmatrix} X_{o d d} & X_e \\ X_{e v e n}^* & \tilde{X} \end{bmatrix}_o \quad (1),$$

where f_k and f_{k+1} are adjacent sub-carriers index. Then the transmitted signal $x_\alpha(n)$ is derived from the inverse Discrete Fourier transform (IDFT) of the encoded symbol $X_\alpha(k)$, $\alpha \in \{R_1, R_2\}$, which can be written as

$$x_\alpha(n) = \frac{1}{\sqrt{N}} \sum_{k=0}^{N-1} X_\alpha(k) \exp\left(\frac{j2\pi nk}{N}\right), \quad -N_g \leq n \leq N-1 \quad (2),$$

where N is the OFDM symbol length, N_g is the length of cyclic prefix (CP).

A multipath channel model taking into account the effects of multiple oscillators is assumed. The discrete-time baseband equivalent asynchronous received signal can be written as

$$y(n) = \sum_{\alpha \in \{R_1, R_2\}} \exp\left(\frac{j2\pi \varepsilon_\alpha n}{N}\right) \sum_{l=0}^{L-1} h_\alpha(l) x_\alpha(n-l) + z(n) \quad (3),$$

where ε_α , $\alpha \in \{R_1, R_2\}$, represents the CFO, which is normalized by the sub-carrier spacing, between the destination node and the relay node α . The l -th path gain profile of the multipath Rayleigh fading channel is denoted as $h_\alpha(l)$, L is the number of multipath. In order to avoid inter-symbol interference (ISI), $N_g \geq L$ should be satisfied. The average total power is normalized such that $E[\sum_{\alpha \in \{R_1, R_2\}} \sum_{l=0}^{L-1} |h_\alpha(l)|^2] = 1$, and $z(n)$ is the AWGN with zero mean and variance σ^2 .

After removing CP and passing through DFT, the received signals on two adjacent subcarriers are

$$\begin{aligned} Y_k &= G_0^{\varepsilon_{R1}} H_{R1,k} X_k + G_0^{\varepsilon_{R2}} H_{R2,k} X_{k+1} \\ &+ \sum_{\substack{m=0 \\ m \neq k}}^{N-1} G_{k,m}^{\varepsilon_{R1}} H_{R1,m} X_{R1,m} + \sum_{\substack{m=0 \\ m \neq k}}^{N-1} G_{k,m}^{\varepsilon_{R2}} H_{R2,m} X_{R2,m} \\ &+ W_k \\ Y_{k+1} &= G_0^{\varepsilon_{R1}} H_{R1,k+1} (-X_{k+1}^*) + G_0^{\varepsilon_{R2}} H_{R2,k+1} X_k^* \\ &+ \sum_{\substack{m=0 \\ m \neq k+1}}^{N-1} G_{k+1,m}^{\varepsilon_{R1}} H_{R1,m} X_{R1,m} + \sum_{\substack{m=0 \\ m \neq k+1}}^{N-1} G_{k+1,m}^{\varepsilon_{R2}} H_{R2,m} X_{R2,m} \\ &+ W_{k+1} \end{aligned} \quad (4),$$

where H_α , $\alpha \in \{R_1, R_2\}$, and W denote the channel response and complex AWGN in the frequency domain. $G_{k,m}^{\varepsilon_\alpha}$ is the ICI coefficient, which destroys orthogonality between sub-carriers, caused by multiple CFOs. It can be defined as

$$\begin{aligned}
G_{k,m}^{\varepsilon_\alpha} &= \frac{1}{N} \sum_{n=0}^{N-1} \exp\left(\frac{j2\pi n(\varepsilon_\alpha - k + m)}{N}\right) \\
&= \frac{\sin(\pi(m - k + \varepsilon_\alpha))}{N \sin(\pi(m - k + \varepsilon_\alpha) / N)} \exp\left(j\pi\left(\frac{N-1}{N}\right)(m - k + \varepsilon_\alpha)\right)
\end{aligned} \tag{5}$$

When $k=m$, $G_{k,m}^{\varepsilon_\alpha}$ can be simply defined as $G_0^{\varepsilon_\alpha}$. Here, the perfect CSI known at the destination node is assumed.

3.2 Multiple CFOs Mitigation

We take cues from the two-step ICI cancellation algorithm for SFBC-OFDM [30] and the two-branch MCFOs mitigation algorithm [29]. Both methods are designed for asynchronous cooperative systems. However, they can only achieve near Alamouti performance with moderate range $[\varepsilon_{\min} - \varepsilon_{\max}]$, in which $\varepsilon_{\max} \leq 0.2$ and the performance degrades rapidly if the MCFOs go beyond the range. We proposed a new SFBC decoding algorithm by better using the separately synchronized signals to extend the tolerance range of multiple CFOs. The detailed mitigation algorithm is described as follows.

As in [29], assume that the receiver can estimate multiple CFOs separately and have multiple copies of the received signal compensated for each CFO. For example, preambles which are orthogonal to each other for each relay node may be used to facilitate the estimation of CFOs. Before DFT, the compensated signal can be express as

$$\tilde{y}_\alpha(n) = \exp(-j2\pi\varepsilon_\alpha n)y(n) \tag{6}$$

where $0 \leq n \leq N-1$ and $\alpha \in \{R_1, R_2\}$. Then, for SFBC, the two sets of separately synchronized signals in the frequency domain can be written as $\tilde{Y}_{R_1}(n) = DFT\{\tilde{y}_{R_1}(n)\}$ and

$$\tilde{Y}_{R_2}(n) = DFT\{\tilde{y}_{R_2}(n)\}.$$

The new SFBC decoding algorithm is modified from the one found in [29] while the major difference is that our algorithm processes two sets of separately synchronized signal jointly, inspired by the method found in [33]. The principle is illustrated in Fig. 3.

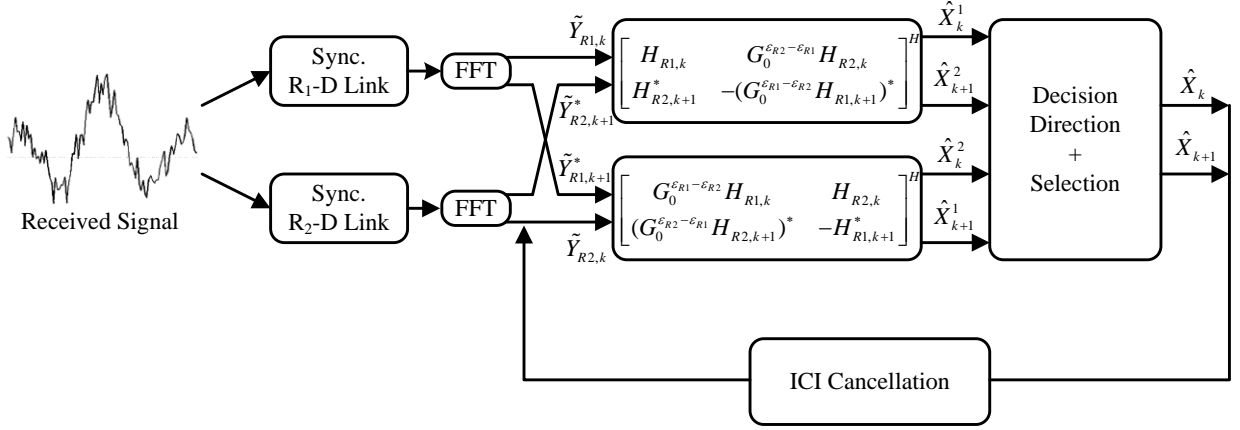


Fig. 9. The block diagram of the receiver with the proposed MCFOs mitigation algorithm

From Fig. 9, we can see that there are two signal sets going into the decision block. Due to synchronization errors, neither of the two signal sets obtained by the SFBC decoding is absolutely better than the other. Signal detection adopts the Minimum Euclidean distance decision rule, as is in [29]: the decoded signal with smaller decision error will be deemed as more reliable and selected. The detection rule can be expressed as

$$\hat{d}_k = \underset{\zeta_i}{\text{arg min}} \left\| \hat{\mathbf{X}}_k^\beta - \zeta \right\|_i \quad (7),$$

Alternatively, to show that the two signal sets indeed possess information to further improve SINR, we propose an ad hoc method which mimics Maximum Ratio Combining (MRC) to combine the two signal sets. Express the signals in a short hand notation:

$$\begin{aligned} \hat{X}_k^1 &= X_k + \Xi_k^1 \\ \hat{X}_k^2 &= X_k + \Xi_k^2 \\ \hat{X}_k^{comb} &= w_k^1 \hat{X}_k^1 + w_k^2 \hat{X}_k^2 \end{aligned} \quad (8),$$

where Ξ_k^1 and Ξ_k^2 are interference plus noise terms. The weights w_k^1 and w_k^2 on the k -th subcarrier are chosen to “maximize” the SINR. Typical MRC solutions are obtained from the optimization problem:

$$\begin{aligned} &\text{minimize } \left\| \mathbf{w}_k^H \Xi_k \right\|^2 \\ &\text{subject to } \mathbf{c}^H \mathbf{w}_k = 1 \end{aligned} \quad (9),$$

in which $\Xi_k = [\Xi_k^1 \ \Xi_k^2]^T$, $\mathbf{w}_k = [w_k^1 \ w_k^2]^T$ and $\mathbf{c} = [1 \ 1]^T$, whose solution is $\mathbf{w}_k = \frac{\mathbf{R}_\Xi^{-1} \mathbf{c}}{\mathbf{c}^H \mathbf{R}_\Xi^{-1} \mathbf{c}}$.

Due to the fact that the interference-plus-noise terms are unknown, we opt to an ad hoc method to calculate \mathbf{w}_k . First, all possible noise-plus-interference terms are calculated by treating every

constellation points as candidate decisions. Then the minimum decision errors in each signal set are selected as the instantaneous noise-plus-interference terms. Then the combining coefficients are obtained via the ratios of instantaneous SINRs. Finally, the decision is made on the combined signal to get \hat{d}_k .

A parallel interference cancellation (PIC) scheme at each sub-carrier finally is added to complete the receiver. Within an iteration, the symbol decisions are used to reconstruct the ICI due to signal spilling from one subcarrier into another. The ICI cancellation operation can be expressed as

$$Y_k^{(r)} = \begin{cases} Y_k & r = 0 \\ Y_k - \sum_{\substack{m=0 \\ m \neq k}}^{N-1} G_{k,m}^{\varepsilon_{R1}} H_{R1,m} \hat{X}_{R1,m}^{(r-1)} - \sum_{\substack{m=0 \\ m \neq k}}^{N-1} G_{k,m}^{\varepsilon_{R2}} H_{R2,m} \hat{X}_{R2,m}^{(r-1)} & r > 0 \end{cases} \quad (10)$$

where $\hat{X}_{R1}^{(r)}$ and $\hat{X}_{R2}^{(r)}$ represent for the symbol decisions of the r -th iteration with the minimum Euclidean distance criterion. As the iteration number increases, more precise estimates of the transmitted symbols can be obtained.

3.3 Time-Frequency Duality and Single-Carrier Systems

Alamouti STBC is a well known transmit diversity scheme for flat fading channels. Since the cooperating nodes are physically separated, the different respective clocks lead to asynchronous transmission and reception. Therefore, the ISI appears and the performance degradation is caused by the non-orthogonal space-time combination. Thanks to time-frequency duality, which ISI caused by STO can be viewed as a time-domain version of ICI, our proposed method is also applicable to single-carrier transmission in the presence of ISI up to a large error range, e.g., $\Delta T_{\max} = 0.625 T_s$, as verified in numerical simulations.

Without going into details, we will summarize the ISI-mitigation steps for single-carrier systems as follows.

- a) The receiver needs to register four values from two separately sampled sequences for one Alamouti block of two transmitted symbols.
- b) Perform two sets of modified Alamouti space-time decoding to reconstruct the nearly orthogonal STBC.
- c) Select the more reliable decoded signal through minimum Euclidean distance decision. Apply iterative Interference cancellation.

3.4 Simulation Results

In this section, we show some simulation results to demonstrate the performance of the proposed scheme for an uncoded cooperative Alamouti SFBC-OFDM system with two relay nodes. The channel used is a four equal gain multipath Rayleigh fading channel (the channel taps are uncorrelated complex Gaussian random variables with zero mean and normalized variance $1/2$). Other simulation parameters are listed in TABLE II.

TABLE II
SIMULATION PARAMETER

Channel Model	Rayleigh Fading
Power Delay Profile	Uniform
Number of Taps	4
Number of Subcarriers	512
Cyclic Prefix	32
Type of Modulation	QPSK
Number of Total Simulated Frame	100000

Fig. 10 depicts the BER vs. bit signal-noise-ratio (E_b/N_0) of the proposed scheme with synchronous impairments. To show the tolerance range to large multiple CFOs, the normalized multiple CFOs are set to be $\varepsilon_{R1} = 0.25$ and $\varepsilon_{R2} = -0.25$. The performance is poor without iterative ICI cancellation. With iterative ICI cancellation, the performance improves, and the full diversity order is achieved. It is also shown that the MRC-like operation can further improve the SINR and the BER approaches the theoretical bound.

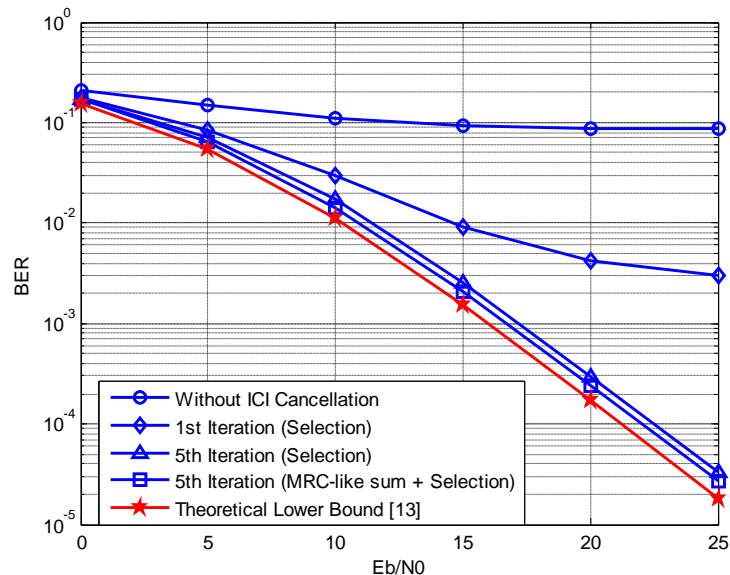


Fig. 10. BER performance with the relative CFO = 0.5

Fig. 11 compares the performance of our algorithm and Zhang's method in [31]. In both cases, iterative ICI cancellation is applied. Zhang's method works fine when multiple CFOs is

less than $[0.2 -0.2]$, but degrades significantly and error floors appear as MCFOs get larger. On the other hand, our proposed receiver maintains the diversity order with a small SNR loss compared to the case with no MCFOs; this confirms that the degradation caused by MCFOs can be effectively reduced even when the offset is large. The effect can be ascribed to the fact that ICI and ISI may be largely eliminated at the SFBC decoding stage.

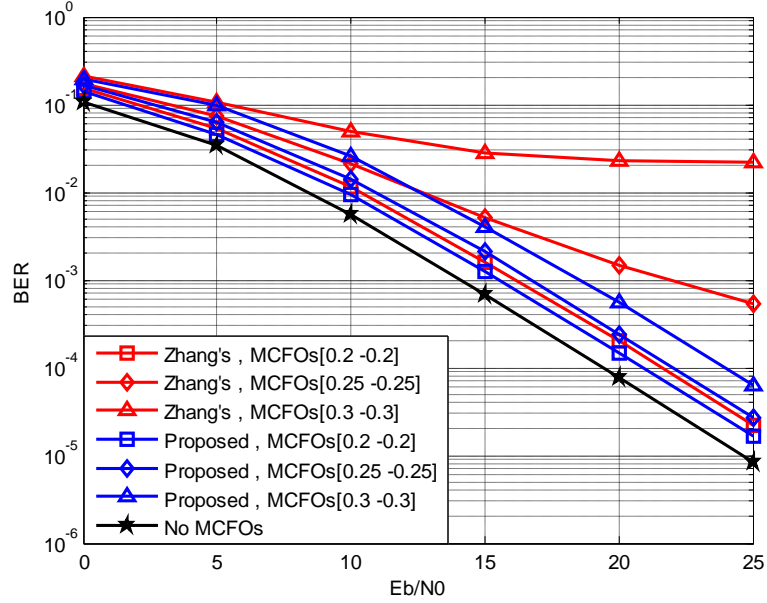


Fig. 11. BER performance comparison between Zhang's method and the proposed algorithm under different multiple CFOs

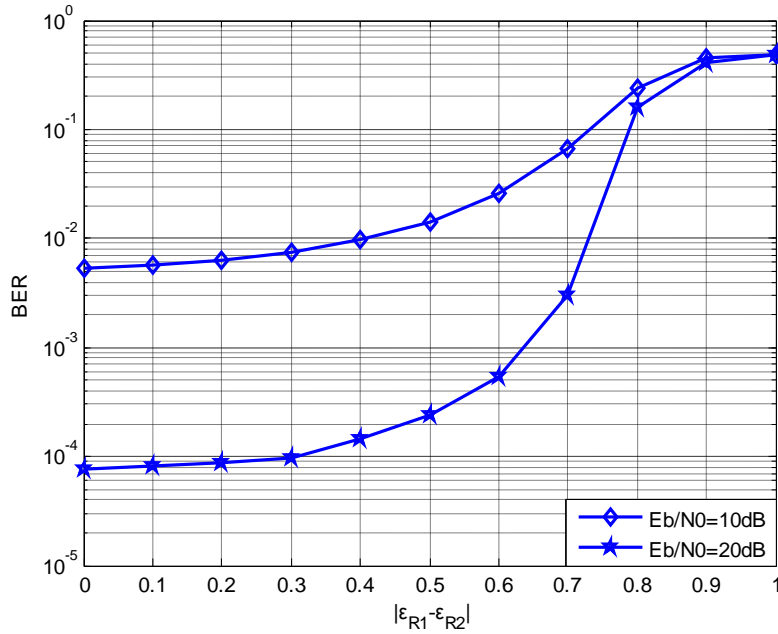


Fig. 12. BER performance vs. relative CFO $|\varepsilon_{R1} - \varepsilon_{R2}|$

Fig. 12 illustrates the BER performance vs. the relative CFO $|\varepsilon_{R1} - \varepsilon_{R2}|$ with $E_b/N_0 = 10$ and 20dB. The increase of relative CFO hurts the performance eventually. However, the Alamouti diversity order can be maintained up to when the relative CFO is 0.6. This shows the superior tolerance to multiple CFOs by deploying our proposed decoding algorithm.

In summary, the performance of distributed SFBC-OFDM systems with the presence of multiple CFOs is studied. A new SFBC decoding algorithm is proposed for cooperative systems to combat multiple CFOs. Iterative interference cancellation is used to further mitigate the ICI and reduce the error floor. Simulation results show that the proposed algorithm is effective for asynchronous cooperative systems. The algorithm has a moderate computational complexity and a superior tolerance range of multiple CFOs, compared to existing techniques. Extension to single-carrier systems with multiple STOs is also outlined.

3. BICM-OFDM to Combat Multiple Synchronous

Errors

In this section, we move on to the second perspective of combating synchronization errors in cooperative MIMO communications. We will view the synchronization errors, not as impairments which cause performance degradation, rather as potential sources of diversity gains. Through careful design of a BICM-based scheme and an iterative receiver, it will be shown that dramatic increase of diversity gain is actually achieved when severe synchronization errors exist.

3.1 System Model

We adopt the decode-and-forward protocol for this section, and BICM-OFDM [24] are chosen as the transmission technique. Fig. 13 shows a generic block diagram of a system employing BICM-OFDM, at the source side the information bits denoted b are first encoded by the outer convolutional encoder and the encoded bits are denoted by $c \in C$, C being the codeword set. The interleaver Π operates on K OFDM symbols of encoded bits with the output denoted by c' , then the inner differential precoder with recursive structure [34] is deployed to enhance overall performance and its output is denoted by d . The resulting bits are mapped into QAM or PSK symbols. The set of constellation points is denoted by χ , as γ bits are mapped into one of 2^γ constellation points according to the mapping rule. After loading the modulated symbols onto active subcarriers, OFDM signal x is generated via N -point IFFT and CP is inserted. The performance depends on the size of interleaver that is γKN bits. Note that the encoded bits are interleaved across several OFDM systems and it is called time-frequency interleaving. The time-domain transmitted signal at Relay Node α can be written as

$$x_\alpha(k) = \frac{1}{\sqrt{N}} \sum_{n=0}^{N-1} \mathbf{X}_\alpha(n) e^{j \frac{2\pi nk}{N}}, \quad N_g \leq k \leq N \quad (11)$$

where $X_\alpha(n)$ is the modulated symbol at the n -th subcarrier, N is the OFDM symbol length, N_g is

the length of CP, k is the sampling index, $\alpha \in \{1, 2, \dots, M\}$ is the relay node index, and M is the number of relays. Assume the CP is longer than the largest channel delay spread plus timing error so that ISI can be ignored.

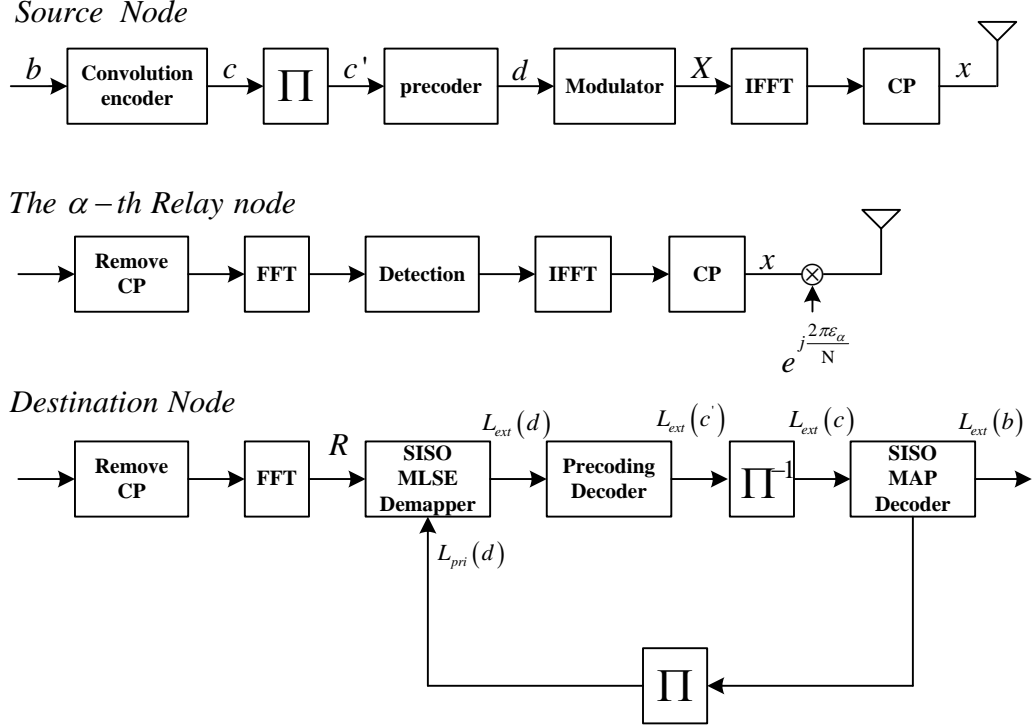


Fig. 13. The block diagram of the proposed scheme for asynchronous cooperative communications

Time varying multipath Rayleigh fading channels are considered, and the discrete time baseband equivalent received signal at the k -th sampling time can be expressed as

$$y(k) = \sum_{\alpha=1}^M e^{j\frac{2\pi\epsilon_{\alpha}k}{N}} \sum_{l=0}^{L-1} h_{\alpha}(k,l)x_{\alpha}(k-l-\tau_{\alpha}) + z(k) \quad (12)$$

where ϵ_{α} and τ_{α} represents the normalize CFO and the timing error between destination node and the α -th relay node. Let $h_{\alpha}(k,l)$ represents the l -th path gain of the multipath Raleigh fading channel from the α -th relay to the destination. The wide-sense stationary uncorrelated scattering (WSSUS) channel is assumed with

$$E[h_{\alpha}^H(k,l)h_{\alpha}(m,l')] = \sigma_h^2 r(q)\delta(l-l') \quad (13)$$

where σ_h^2 denotes the variance of the l -th tap gain with normalized average power

$E[\sum_{\alpha=1}^M \sum_{l=1}^{L-1} |h_{\alpha}(h,l)|^2] = \sum_{\alpha=1}^M \sigma_h^2 = 1$, L is the number of multipath, $r(q)$ denotes the normalized tap autocorrelation ($r(0)=1$), and $\delta(l-l')$ is the Kronecker delta function. Moreover, assume the paths are subject to Rayleigh fading, so that

$$r(q) = J_0(2\pi f_\alpha (k - m)T) \quad (14)$$

where $J_0(\cdot)$ denotes the zero-order Bessel function of the first kind and f_α is the Doppler frequency of the α -th relay node, T represents one OFDM symbol time, $x_\alpha(k)$ is the transmitted signal of the α -th relay node, and $w(k)$ is additive noise, which is independently and identically distributed (i.i.d.) complex Gaussian random variable with zero mean and variance σ_z^2 . Consider the model in frequency domain by taking the N -point DFT to $y(k)$ in (2). The p -th OFDM symbol in the frequency received signal can be written be

$$\begin{aligned} \mathbf{R}_p &\triangleq \mathbf{F}^H y(k) \\ &= \sum_{\alpha=1}^M \mathbf{F}^H \mathbf{E}_{\alpha,p} \mathbf{H}_{\alpha,p} \mathbf{F} \mathbf{X}_p + \mathbf{Z}_p \\ &= \sum_{\alpha=1}^M \mathbf{T}_{\alpha,p} \mathbf{G}_{\alpha,p} \mathbf{X}_p + \mathbf{Z}_p \\ &= \sum_{\alpha=1}^M \tilde{\mathbf{G}}_{\alpha,p} \mathbf{X}_p + \mathbf{Z}_p, \quad p = 1, 2, \dots, K \end{aligned} \quad (15)$$

where $\mathbf{R}_p \triangleq [\mathbf{R}_{N_p}, \mathbf{R}_{N_p+1}, \dots, \mathbf{R}_{N_p+N-1}]^T$ is an $N \times 1$ frequency domain receiver vector, $N_p = (p-1)N$ denotes the starting index of each OFDM symbol, $\mathbf{F} = 1/\sqrt{N} \exp\{j2\pi nk/N\}$ is $N \times N$ the IDFT matrix with (n,k) , the entry $[\mathbf{F}]_{n,k} = 1/\sqrt{N} \exp\{j2\pi(k-1)(n-1)/N\}$, $n = 1, 2, \dots, N$, $\mathbf{X}_p = \mathbf{F}^H x(k)$ and $\mathbf{Z}_p = \mathbf{F}^H z(k)$ are the frequency domain transmitted data and additive noise, respectively, where \mathbf{X}_p and \mathbf{Z}_p are an $KN \times 1$ vector. Since FFT is unitary, the entries of \mathbf{Z}_p are still white complex Gaussian variables with mean zero and variance σ_z^2 .

3.2 The Receiver Algorithm

For the receiver, both MSE and MLSE equalizers can be used. Here we focus on the design of MLSE receiver in the frequency domain and the overall receiver. The iterative receiver consists of a Soft-Input Soft-Output (SISO) MLSE demapper/equalizer and Maximum A Posterior (MAP) decoders for both the precoder and the convolutional encoder. The soft outputs are typically represented by the log-likelihood ratio (LLRs). The signal detection in the demapper/equalizer is carried out with MLSE.

The task of the equalizer is to estimate the transmitted \mathbf{X} based on the received observations \mathbf{R} . more specifically, the maximum likelihood sequence estimation is to choose that sequence of symbols $\mathbf{X} = \{x_1, x_2, \dots, x_K\}$ that maximizes the likelihood of the received sequence of observation $\mathbf{R} = \{\mathbf{R}_1, \mathbf{R}_2, \dots, \mathbf{R}_K\}$, i.e., maximizes the joint conditional probability the $P(\mathbf{R}|\mathbf{X})$. the obtained

sequence is the optimal solution and procedure is referred to as MLSE. There exist basic approaches to implement an MLSE equalizer in [35].

Start with the states at the k -th stage of the associated trellis diagram that are related to the $Q-1$ most recent transmitted symbols, i.e.,

$$s_k \rightarrow (x_{\langle -D+k \rangle_N}, x_{\langle -D+k+1 \rangle_N}, \dots, x_k, \dots, x_{\langle D+k-1 \rangle_N}) \quad (16)$$

Thus, each state corresponds to one of the $2^{\gamma(Q-1)}$ possible vectors that can be formed from $Q-1$ symbols. There are 2^γ allowable transitions that emerge from a state s_k and terminate at 2^γ different states s_{k+1} , leading to a total of $2^{\gamma Q}$ transition branches connecting two successive states ($s_k \rightarrow s_{k+1}$). Each transition is associated with a cost, contributing to the total cost of a path along the states. The cost of the i -th transition between s_k and s_{k+1} exists transition probabilities is called a branch metric, connecting two specific consecutive states ($s_k \rightarrow s_{k+1}$), is given by

$$\gamma_i(s_k \rightarrow s_{k+1}) = -\frac{1}{2\sigma_z^2} |\mathbf{R}_k - \bar{\mathbf{G}}\mathbf{X}|^2 \quad (17)$$

Notice that each state has 2^γ incoming branches except a few stages in the beginning and in the end. Each incoming branch is due to the advent of a new symbol. Of the 2^γ incoming branches, only the one connected, and the new symbol metric $\Gamma(s_k)$ is calculated that formulation represent

$$\Gamma(s_k) = \Gamma(s_{k-1}) + \gamma_i(s_k \rightarrow s_{k+1}) + \sum_{n'=1}^{\gamma} L_{MLSE}^{pri}(d_k^{n'}) \lambda^{n'}(x) \quad (18)$$

where $L_{MLSE}^{pri}(\bullet)$ is priori bit LLRs by the SISO outer decoder and $\lambda^{n'}(x)$ is represent the constellation point x of the value at the n' -th bit. That retained path is referred to as survivor path. After all states of the trellis have been gone through, the smallest state metric be found and trace back that the $\hat{\mathbf{x}}$ is obtained.

A soft decision as the log-likelihood ratio is obtained by

$$L(d_k) = \ln\left(\frac{P(\hat{d}_k = 1 | \mathbf{R})}{P(\hat{d}_k = 0 | \mathbf{R})}\right) \quad (19)$$

Thus MLSE output bit LLRs is transformed by symbol metric.

$$\begin{aligned} L_{MLSE}(d_k^n) &= \ln \sum_{\mathbf{X} \in \mathcal{X}_1^n} P(\mathbf{R}(k) | \bar{\mathbf{G}}, \mathbf{X}) \\ &\quad - \ln \sum_{\mathbf{X} \in \mathcal{X}_0^n} P(\mathbf{R}(k) | \bar{\mathbf{G}}, \mathbf{X}) \\ &\quad - L_{MLSE}^{pri}(d_k^n) \end{aligned} \quad (20)$$

where d_k^n represent n -th bit at k -th transmit subcarrier is mapped, \mathcal{X}_b^n represent constellation point set of n -th bit is $b \in \{0,1\}$. The inner and outer decoder are adopting a maximum a posterior probability (MAP), output are the bit log likelihood ratio and log-MAX algorithm is usually applied for lower computational complexity. A trade-off between complex and performance can be achieved by different choices of D , K , and γ .

The computational complexity of MLSE is $\mathcal{O}(IN2^Q)$ where I is number of iteration and for the MMSE receiver it is $\mathcal{O}(N^3)$ in one OFDM symbol. The MLSE is much more expensive than the MMSE receiver when high order modulation or large D is used.

3.3 Simulation Results and Discussion

To demonstrate the effectiveness of the MLSE receiver, Monte Carlo simulations are carried out, and we compare the Bit Error Rate (BER) performance between the MLSE equalizer and MMSE equalizer. Notice that both receivers effectively harvest the extra diversity gain provided by synchronization errors.

We consider a BICM-OFDM system with $N = 64$, CP length = 8, and 4-QAM modulation. A two-path wide-sense stationary uncorrelated scattering (WSSUS) Rayleigh fading channel (generated using Jakes Model) between any relay nodes and each relay are equal power, the convolutional code uses $\mathbf{G}(D)=(1+D^2, 1+D+D^2)$ as the generator polynomial, and $G(D)=1/(1+D^2)$ is the generator polynomial for the precoder. One frame consists of 10 OFDM symbols. Furthermore, perfect estimations of MCFOs and channel matrices are assumed.

Fig. 14 shows the BER performance versus SNR for the comparison between conventional MMSE equalizer, traditional 1-tap equalizer and the MLSE equalizer in synchronous impairments. For the simulation, normalized Doppler frequency $fd=0.001$ is employed at both relays, the normalized MCFOs are 0.2 and -0.2. With the large MCFOs, the 1-tap equalizer suffers an obvious error floor.

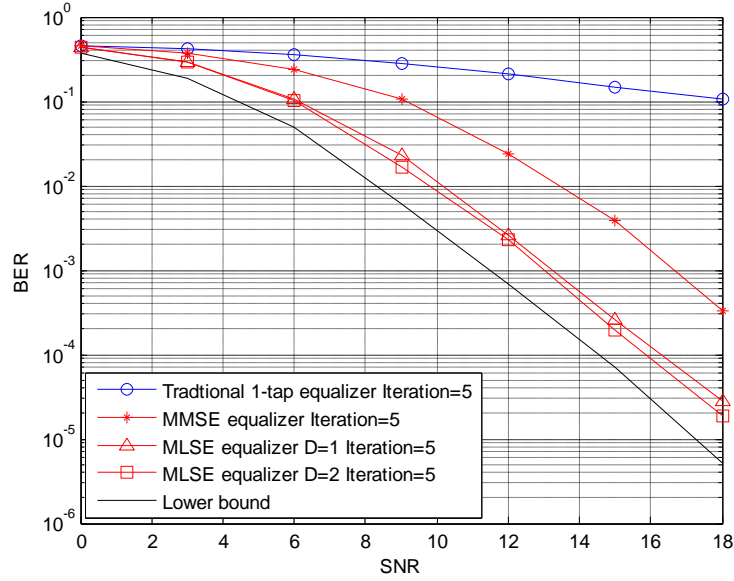


Fig. 14. BER comparison between MMSE equalizer, 1-tap equalizer and MLSE equalizer in the cooperative communication

On contrast, the MLSE equalizer not only successfully compensates for the ICI but also obtain an SNR gain about 3dB. The benefits of SNR gain, we can via SINR to explicit explanation and the derivation in appendix. The optimal solution is joint processing of demodulation and decoding is considered, which lead to approach low bound. Notice that with both equalizers the system achieves full diversity.

Fig. 15 shows the results for the two relay nodes and three relay nodes. It can be seen from the figure that as the number of relay increases in the systems, the diversity order of distributed BICM-OFDM increases up to the maximum diversity of $\min\{M \times r \times T \times L, d_{\text{free}}\}$. It can be observed that the tree relays case has a diversity order of 5 and the BER curve is steep.

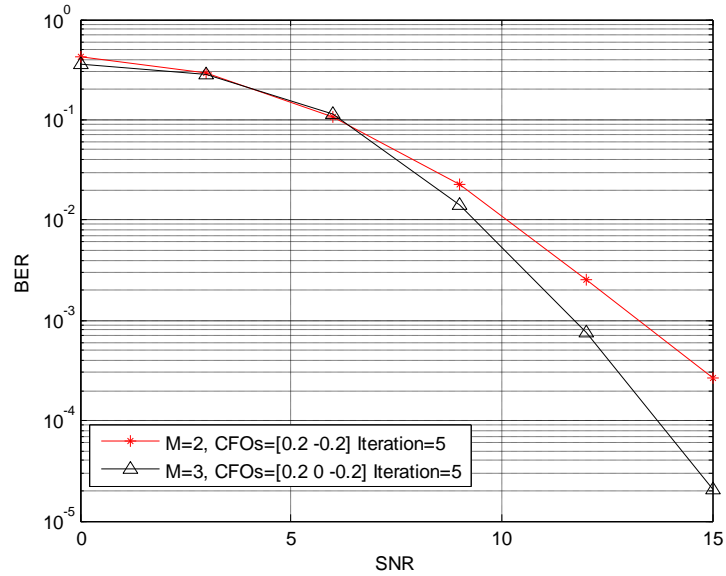


Fig. 15. The BER curves compared with difference number of relay nodes

In Fig. 16, all the realistic synchronous impairments are considered. The timing errors is [0 3], normalized Doppler frequency is 0.1 for both relays and MCFOs is [0.2 -0.2]. In our proposed the performance show efficiently collects the diversity form time diversity due to the Doppler effect, frequency diversity due to timing error and special diversity converted to time diversity due to MCFOs. It observed that the diversity is more than four.

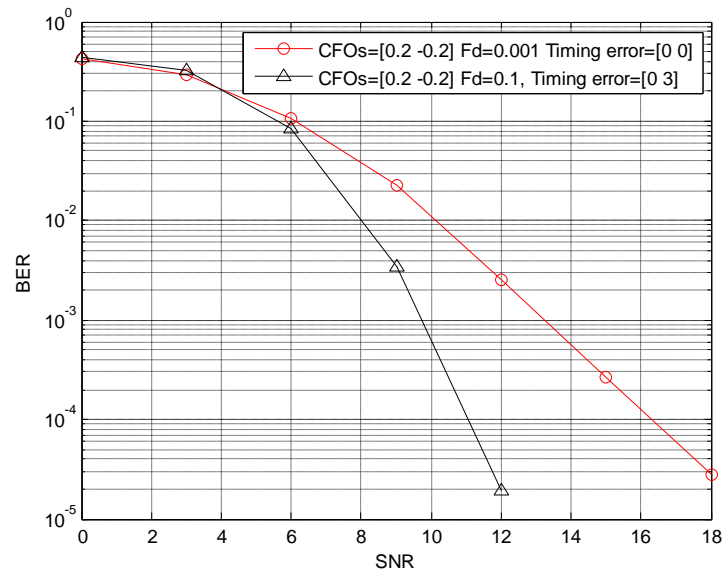


Fig. 16. The BER for cooperative communication under time error = [0 3], normalize Doppler frequency = 0.1, MCFOs = [0.2 -0.2]

In summary, BICM has the potential to improve performance with relatively ease in many OFDM wireless communication systems. It is shown that, with proper receiver design, the BICM-OFDM can be effective to combat synchronous errors as well as harvest potential diversity gain in cooperative communications. Typical BICM-OFDM systems suffer error floors due to ICI caused by MCFOs and Doppler effects. To deal with such a problem, we propose an

MLSE-based frequency domain equalizer combined with a turbo decoder to break the error floor. The proposed approach has excellent BER performance, and it is flexible in a way that extension to more relays for improvement in diversity gain is straightforward. The complexity is a big problem in the receiver if D is greater than three, and future research in the complexity reduction will be considered.

4. 結果與討論

寬頻合作式無線多輸出入通訊系統如果運行在一高速移動環境中，因都普勒效應及多重同步誤差所造成的通道衰落及載波間干擾問題，將造成嚴重的系統效能損失，大大地降低了這類方法的實用性。在高速移動問題方面，我們探討了載波間干擾問題，瞭解到具成本效益與良好表現的方法仍為業界急需，我們從實用角度出發，重新檢視現有方法的侷限，並提出新的解決方案，同時我們的通道模型也非常適合寬頻合作式無線多輸出入通訊系統的通道估測需求。

在同步問題方面，合作式通訊系統和一般習見的情況有所不同、同步問題在傳送端便已存在。互相合作形成天線陣列也許分散在極為不同的傳輸環境中，因而無法像傳統處於同一地點的傳送天線陣列達成載波頻率及符元時間的完全同步。本計畫預計經由兩個面向提出同步問題的解決方案。首先我們從設計接收機著手，我們考慮廣泛使用的阿拉木提多輸出入系統，為其設計一套對同步誤差具有超強容忍力的接收機，數值模擬結果表明它運用於單載波系統可抵抗極大的載波頻率誤差，運用於多載波系統則可抵抗極大的符元時間誤差。

其次、我們也從編碼設計的角度解決同步問題。在這裡，我們不將同步誤差視做必須避免的問題，反而視為多集性增益的可能來源。經由為合作式多輸出入通訊設計一種位元交錯編碼調變方式，我們發現、當同步誤差存在時、多集性增益竟大幅增加，我們也對此結果做了一些理論分析。至此、在 Alamouti 編碼以及 BICM 的情況下之同步問題，已獲得解決。

5. 計劃成果自評

總結我們的技術成果，在於解決合作式通訊(分散式多輸出入系統 distributed MIMO)在搭配 Alamouti 編碼或是 BICM 的情況下之同步問題，以及高速移動下可能面臨的載波間干擾問題。我們提出一個可評估載波間干擾嚴重性並隨時調整的處理架構，有效降低了運算成本，確實為業界所需之實用性技術。我們也發展了兩套傳輸架構，兩者皆有極佳的同步

誤差容忍度，在文獻中尚未見到有可和我們比肩的結果。我們認為，這項成果，對合作式多輸出入系統的實用化有很大的意義，唯目前開發的接收機演算法仍具高複雜度，降低運算複雜度我們努力的方向。

在論文發表方面，累計相關國際會議論文發表五篇(其中兩篇與林大衛教授合作)[36]-[40]，已有三篇會議論文轉為期刊論文投稿，但過程未如人意，目前尚在審稿中。

6. 參考文獻

- [1] 最新標準資料可在 <http://www.3gpp.org/ftp/Specs/latest/> 下載。
- [2] WiMAX Forum, *Mobile WiMAX — Part I: A Technical Overview and Performance Evaluation*. WiMAX Forum White Paper, Aug. 2006.
- [3] *IEEE Standard for Local and Metropolitan Area Networks – Part 16: Air Interface for Fixed and Mobile Broadband Wireless Access Systems – Multihop Relay Specification*.
- [4] R. Irmer *et al.*, “Coordinated multipoint: concepts, performance, and field trial results,” *IEEE Comm. Magazine*, pp. 102-111, no. 2, Feb. 2011.
- [5] W. G. Jeon, K. H. Chang, and Y. S. Cho, “An equalization technique for orthogonal frequency-division multiplexing systems in time-variant multipath fading channels,” *IEEE Trans. Commun.*, vol. 47, no. 1, pp. 27–32, Jan. 1999.
- [6] A. Stamoulis, S. N. Diggavi, and N. Al-Dhahir, “Intercarrier interference in MIMO OFDM,” *IEEE Trans. Signal Process.*, vol. 50, no. 10, pp. 2451–2464, Oct. 2002.
- [7] X. Cai and G. B. Giannakis, “Bounding performance and suppressing intercarrier interference in wireless mobile OFDM,” *IEEE Trans. Commun.*, vol. 51, no. 12, pp. 2047–2056, Dec. 2003.
- [8] A. Gorokhov and J.-P. Linnartz, “Robust OFDM receivers for dispersive time-varying channels: equalization and channel acquisition,” *IEEE Trans. Wireless Commun.*, vol. 52, no. 4, pp. 572–583, Apr. 2004.
- [9] P. Schniter, “Low-complexity equalization of OFDM in doubly selective channels,” *IEEE Trans. Signal Process.*, vol. 52, no. 4, pp. 1002–1011, Oct. 2004.
- [10] I. Barhumi, G. Leus, and M. Moonen, “Time-domain and frequency-domain per-tone equalization for OFDM over doubly selective channels,” *Signal processing*, vol. 84, no. 11, pp. 2055–2066, 2004.
- [11] Y. Mostofi and D. C. Cox, “ICI mitigation for pilot-aided OFDM mobile systems,” *IEEE Trans. Wireless Commun.*, vol. 4, no. 2, pp. 765–774, Mar. 2005.
- [12] L. Rugini, P. Banelli, and G. Leus, “Simple equalization of time-varying channels for OFDM,” *IEEE Commun. Lett.*, vol. 9, no. 7, pp. 619–621, Jul. 2005.

- [13] S. Das and P. Schniter, "Max-SINR ISI/ICI-shaped multi-carrier communication over the doubly dispersive channel," *IEEE Trans. Signal Process.*, vol. 55, no. 12, pp. 5782–5795, Dec. 2007.
- [14] D. N. Liu and M. P. Fitz, "Iterative MAP equalization and decoding in wireless mobile coded OFDM," *IEEE Trans. Commun.*, vol. 57, no. 7, pp. 2042–2051, Jul. 2009.
- [15] C.-Y. Hsu and W.-R. Wu, "Low-complexity ICI mitigation methods for high-mobility SISO/MIMO-OFDM systems," *IEEE Trans. Veh. Technol.*, vol. 58, no. 6, pp. 2755–2768, Jul. 2009.
- [16] I. Barhumi and M. Moonen, "MLSE and MAP equalization for transmission over doubly selective channels," *IEEE Trans. Veh. Technol.*, vol. 58, no. 8, pp. 4120–4128, Oct. 2009.
- [17] H.-W. Wang, D.-W. Lin, and T.-H. Sang, "OFDM signal detection in doubly selective channels with whitening of residual intercarrier interference and noise," in *Proc. IEEE VTC-Spring*, May 2010.
- [18] A. Sendonaris, E. Erkip, and B. Aazhang, "User cooperative diversity part I: system description," *IEEE Trans. Commun.*, vol. 51, no. 11, pp. 1927-1938, Nov. 2003.
- [19] A. Sendonaris, E. Erkip, and B. Aazhang, "User cooperative diversity part II: implementation aspects and performance analysis," *IEEE Trans. Commun.*, vol. 51, no. 11, pp. 1939-1948, Nov. 2003.
- [20] W. Roh and A. Paulraj, "MIMO channel capacity for the distributed antenna," *Proc. VTC 2002-Fall*, Vol. 2, pp. 706 – 709, 2002.
- [21] L. Xiao, L. Dai, H. Zhuang, S. Zhou, and Y. Yao, "Information-theoretic capacity analysis in MIMO distributed antenna systems," *Proc. 2003. VTC 2003-Spring*, Vol. 1, pp. 779 – 782, 2003.
- [22] S. K. Jayaweera, "Virtual MIMO-based cooperative communication for energy-constrained wireless sensor networks," *IEEE Trans. Wireless Communications*, Vol. 5 , pp. 984 – 989, May 2006.
- [23] S. M. Alamouti, "A simple transmit diversity technique for wireless communications," *IEEE J. Select. Areas Commun.*, vol. 16, pp. 1451-1458, Oct. 1998.
- [24] G. Caire, G. Taricco, and E. Biglieri, "Bit-interleaved coed modulation," *IEEE Trans. Inf. Theory*, vol. 44, no. 3, pp. 927-946, May 1998.
- [25] F. Tian, X.-G. Xia, and P. C. Ching, "Equalization in space-frequency coded cooperative communication system with multiple frequency offsets," *IEEE ISSCS*, vol. 2, pp. 1-4, July. 2007.
- [26] Z. Li, D. Qu, and G. Zhu, "An equalization technique for distributed STBC-OFDM system with multiple carrier frequency offsets," in *Proc. IEEE WCNC'06*, vol. 2, pp. 839-843, Apr. 2006.
- [27] Q. Huang, M. Ghogho, and J. Wei, "Data detection in cooperative STBC-OFDM systems with multiple frequency offsets," *IEEE Signal Proc. Letters*, vol. 16, pp. 600-603, July.

2009.

- [28] Z. Li and X.-G. Xia, "An Alamouti coded OFDM transmission for cooperative systems robust to both timing errors and frequency offsets," *IEEE Trans. Wireless Commun.*, vol. 7, no. 5, pp. 1839-1844, May. 2008.
- [29] Y. Zhang, "Multiple CFOs compensation and BER analysis for co-operative communication systems," in *Proc. IEEE WCNC'09*, pp. 1-6, Apr. 2009.
- [30] D. Sreedhar and A. Chockalingam, "ICI-ISI mitigation in cooperative SFBC-OFDM with carrier frequency offset," in *Proc. IEEE PIMRC'07*, pp. 1-5, Sept. 2007.
- [31] W. Zhang, D. Qu, and G. Zhu, "Performance investigation of distributed STBC-OFDM system with multiple carrier frequency offsets," in *Proc. IEEE PIMRC'06*, pp. 1-5, Sept. 2006.
- [32] J. N. Laneman and W. Wornell, "Distributed space-time-coded protocols for exploiting cooperative diversity in wireless networks," *IEEE Trans. Inform. Theory*, vol. 49, pp. 2415-2425, Oct. 2003.
- [33] T. D. Nguyen, O. Berder, and O. Sentieys, "Efficient space time combination technique for unsynchronized cooperative MISO transmission," *IEEE VETECS'08*, pp. 629-633, May. 2008.
- [34] I. Lee, "The effect of a precoder on serially concatenated coding systems with an ISI channel," *IEEE Trans. Commun.*, vol.49, no. 7, pp. 1168-1175, Jul 2001.
- [35] G. E. Bottomley and S. Chennakeshu, "Unification of MLSE receivers and extension to time-varying channels," *IEEE Trans. Commun.*, vol. 46, pp. 464-472, Apr 1998.
- [36] Hsin-De Lin, Tzu-Hsien Sang, and David W. Lin, "BICM-OFDM for cooperative communications with multiple synchronization errors," accepted by IEEE IWCMC 2010.
- [37] Yu-Feng Chou and Tzu-Hsien Sang, "Efficient interpolation of precoding matrices in MIMO-OFDM systems," accepted by IEEE SPAWC 2010.
- [38] Hai-Wei Wang, David W. Lin, and Tzu-Hsien Sang, "OFDM signal detection in doubly selective channels with whitening of residual intercarrier interference and noise," IEEE VTC2010-Spring.
- [39] Tsung-Ta Lu, Hsin-De Lin, and Tzu-Hsien Sang, "An SFBC-OFDM Receiver to Combat Multiple Carrier Frequency Offsets in Cooperative Communications," submitted to IEEE PIMRC 2010.
- [40] Tzu-Hsien Sang and Hsin-Hua Huang, "EVM simulation of power amplifiers with designed signals in OFDM systems," ICEICE 2011, 2011.

國科會補助專題研究計畫項下出席國際學術會議心得報告

日期：100年8月26日

計畫編號	NSC 99-2219-E-009 -009		
計畫名稱	寬頻合作式無線多輸出入通訊系統--子計畫二：合作式多輸出入下行考慮同步不確定之傳收器設計(2/2)		
出國人員姓名	桑梓賢	服務機構及職稱	國立交通大學電子工程學系助理教授
會議時間	99年9月26日至 99年9月30日	會議地點	土耳其伊斯坦堡
會議名稱	(中文) 2010年個人、室內、行動無線通訊研討會 (英文) IEEE Symposium on Personal, Indoor, and Mobile Radio Communications		
發表論文題目	(中文) 一個可用於合作式通訊中對抗多重載波頻率偏移的空時區塊碼-正交頻率多工接收機 (英文) An SFBC-OFDM Receiver to Combat Multiple Carrier Frequency Offsets in Cooperative Communications		

一、參加會議經過

IEEE PIMRC 在無線通訊領域雖不是頂尖、也算是較知名的會議。本次參加會議、除了 keynote speech 和一般技術論文發表的場次，也著重參與各類 panel discussion，並積極與業界工程師們交流，希望進一步瞭解實務上大家對無線通訊發展方向的想法。

我的論文安排在 29 號早上之 MIMO III session，很遺憾場地聲學狀況不理想，講者和聽眾之間交流並不順利，也警惕我是否演講題目並未引起廣泛興趣？我在發表後也同幾位聽眾交流，發現本場次聽眾背景較雜、應與論文題目不統一有關。

幾場 Panel discussion 皆緊扣當前發展熱點，聽眾參與熱情高漲，討論很盛，我也問了兩個問題，獲益頗豐，於下節與會心得中詳述。

二、與會心得

在一般技術論文方面，歷眼所見、較無突破性的發展，以遞增性(incremental)研究為多，本人論文很慚愧地似也在此列。我原先認為、在合作式通訊中，多重載波頻率偏移將是無法迴避且亟待解決的問題、應有不錯的反響，但似乎大家認為這只是一個常規且必能解決的問題，但這又與我後來在 panel discussion 及與若干工程師聊天得到的印象不大一致。總而言之、我想我的論文完成度還不夠，應用範圍也要再加強，還要再發掘其潛力。

在某場 panel discussion 中，討論了 femto cell 是否不會流行？與會者多認為如此， femto cell 只會在 niche market 存在，而異網融合會是更容易走的路。相反的，coordinated multipoint (簡稱 CoMP) 仍然看好，我當然同意此一結論，因為我的論文，便是在 CoMP 內去解決多重載波頻率偏移問題一個很簡單而有效的作法。另一場 panel 討論了 social media communications ，雖然較無具體結論但也讓人眼睛一亮。

我也積極與業界人士交流，某 Broadcom 工程師告訴我， CoMP 前景看好，但目前大家發展重點還在大題目上，多重載波頻率偏移是一個重要但小的問題，將來一定有解、不急。這是業界的心態，我也可以理解。

另、我與林大衛教授也共同發表了一篇關於中繼站的最佳放大策略的論文，頗受聽眾歡迎，這也反映了目前無論 relay 或 CoMP 仍以研究“大”問題為主，還未注意到 PHY 層的技术細節。要做一流研究，還是得回到“大”問題，人家能跟著做的題目，才會受到重視。

三、考察參觀活動(無是項活動者略)

無

四、建議

無

五、攜回資料名稱及內容

大會光碟及議程手冊

六、其他

(論文接受函及論文摘要)

寄件者: "Hakan Delic" <delic@boun.edu.tr> 主旨: [PIMRC 2010 Track 1] Your paper #1569310623 has been accepted 日期: Mon, 五月 24, 2010 4:33 am 收件者: "Tsung-Ta Lu" <pignose.ee96g@g2.nctu.edu.tw> 副本: "Hsin-De Lin" <good.ee92g@nctu.edu.tw>,"Tzu-Hsien Sang" <tzuhsien54120@faculty.nctu.edu.tw>

Dear Mr. Tsung-Ta Lu:

Congratulations - your paper #1569310623 ('An SFBC-OFDM Receiver to Combat Multiple Carrier Frequency Offsets in Cooperative Communications') for PIMRC 2010 Track 1 has been accepted and will be presented in the session titled .

The reviews are below or can be found at <http://edas.info/showPaper.php?m=1569310623>.

Regards,

Stefan Kaiser, Mutlu Koca, Geert Leus, Heidi Steendam

PIMRC 2010 Track 1 Co-Chairs

Abstract — In this paper, a new space-frequency combination technique is proposed for Alamouti coded Orthogonal Frequency Division Multiplexing (OFDM) in the context of cooperative communications. Since cooperative antennas are distributed, there may exist multiple carrier frequency offsets (MCFOs) which cause problems for conventional space-frequency decoding. The proposed algorithm, taking cues from existing MCFO-compensating algorithms [13][19], combines two sets of separately synchronized signal to mitigate inter-carrier interference (ICI). Iterative interference cancellation and a maximum-ratio-combining-like technique are also deployed to further improve performance with low computational complexity. It is observed that the proposed method achieves better bits error rate (BER) performance and has a superior tolerance of multiple CFOs, compared to existing methods.

國科會補助計畫衍生研發成果推廣資料表

日期:2011/08/31

國科會補助計畫	計畫名稱: 子計畫二: 合作式多輸出入下行考慮同步不確定之傳收器設計(2/2)		
	計畫主持人: 桑梓賢		
	計畫編號: 99-2219-E-009-009-		學門領域: 接取技術(網通國家型)
研發成果名稱	(中文) 適用於3GPP LTE之時脈同步及細胞搜索方法		
	(英文) A timing synchronization and cell search method for 3GPP LTE		
成果歸屬機構	國立交通大學	發明人 (創作人)	桑梓賢, 蔡耀賢
	<p>(中文) 這個發明主要提出一個好的時間同步方法和初始細胞搜索流程, 應用於以OFDMA技術為基礎的無線通訊系統, 例如3GPP長期技術演進(LTE)標準。初始細胞搜索流程主要分成四個步驟, 第一步驟必須將接收端所接收到的訊號, 經過低通濾波器將同步訊號以外的訊號濾掉; 第二步驟執行時間同步, 利用第二同步訊號的對稱性, 對載波頻域偏差較不敏感的特性, 可以提高時間同步的準確性, 找出第二同步訊號(而非如一般去找主同步訊號)的起始點; 第三步驟利用找到的第二同步訊號的起始點, 經過結合循環字首盲檢測與主同步訊號偵測得到主同步訊號的位置和細胞第二編號(), 並解決載波頻率偏移問題, 第四步驟則是利用所得到的細胞第二編號進行第二同步訊號的偵測, 得到細胞第一編號(), 藉由結合第一編號與第二編號, 可以得到完整的細胞編號, 細胞搜索也就此完成。</p> <p>(英文) The invention is a novel timing synchronization method and cell search procedure for wireless communication systems based on OFDMA, such the 3GPP LTE. The procedure can be divided into four steps. First, the received signal is passed through a low-pass filter to remove signals outside the interested band. Second, timing synchronization is performed by examining SSS's self symmetric correlation that is immune to carrier frequency offsets. The property can improve the accuracy of timing synchronization. Third, in time or in frequency domain, using the detected SSS initial position to facilitate the joint blind detection of cyclic prefix and PSS for finding out the CP length, PSS position and . The CFO problem can also be solved in this step. Finally, SSS detection is conducted. After going through the procedure the physical-layer Cell-ID is obtained and cell search is accomplished.</p>		
產業別	電信工程業		
技術/產品應用範圍	4G手機		
技術移轉可行性及預期效益	LTE 是4G手機最重要的標準, 預期前景非常廣大, 本案提出解決LTE同步問題非常有效率的作法、深具應用價值。		

註: 本項研發成果若尚未申請專利, 請勿揭露可申請專利之主要內容。

99 年度專題研究計畫研究成果彙整表

計畫主持人：桑梓賢		計畫編號：99-2219-E-009-009-					
計畫名稱：寬頻合作式無線多輸出入通訊系統--子計畫二：合作式多輸出入下行考慮同步不確定之傳收器設計(2/2)							
成果項目		量化			單位	備註（質化說明：如數個計畫共同成果、成果列為該期刊之封面故事...等）	
		實際已達成數（被接受或已發表）	預期總達成數(含實際已達成數)	本計畫實際貢獻百分比			
國內	論文著作	期刊論文	0	0	100%	篇	
		研究報告/技術報告	0	0	100%		
		研討會論文	0	0	100%		
		專書	0	0	100%		
	專利	申請中件數	2	2	100%	件	一件已通過校內評審 一件剛提案
		已獲得件數	0	0	100%		
	技術移轉	件數	0	0	100%	件	
		權利金	0	0	100%	千元	
	參與計畫人力（本國籍）	碩士生	4	4	100%	人次	
		博士生	1	2	50%		
		博士後研究員	0	0	100%		
		專任助理	0	0	100%		
國外	論文著作	期刊論文	0	2	0%	篇	已有3篇國際會議論文轉成期刊論文投稿中 應能達成最終2篇的目標
		研究報告/技術報告	0	0	100%		
		研討會論文	5	5	100%		
		專書	0	0	100%		
	專利	申請中件數	0	0	100%	件	
		已獲得件數	0	0	100%		
	技術移轉	件數	0	0	100%	件	
		權利金	0	0	100%	千元	
	參與計畫人力（外國籍）	碩士生	0	0	100%	人次	
		博士生	0	0	100%		
		博士後研究員	0	0	100%		
		專任助理	0	0	100%		

<p>其他成果 (無法以量化表達之成果如辦理學術活動、獲得獎項、重要國際合作、研究成果國際影響力及其他協助產業技術發展之具體效益事項等，請以文字敘述填列。)</p>	<p>無</p>
--	----------

	成果項目	量化	名稱或內容性質簡述
科 教 處 計 畫 加 填 項 目	測驗工具(含質性與量性)	0	
	課程/模組	0	
	電腦及網路系統或工具	0	
	教材	0	
	舉辦之活動/競賽	0	
	研討會/工作坊	0	
	電子報、網站	0	
	計畫成果推廣之參與(閱聽)人數	0	

國科會補助專題研究計畫成果報告自評表

請就研究內容與原計畫相符程度、達成預期目標情況、研究成果之學術或應用價值（簡要敘述成果所代表之意義、價值、影響或進一步發展之可能性）、是否適合在學術期刊發表或申請專利、主要發現或其他有關價值等，作一綜合評估。

1. 請就研究內容與原計畫相符程度、達成預期目標情況作一綜合評估

達成目標

未達成目標（請說明，以 100 字為限）

實驗失敗

因故實驗中斷

其他原因

說明：

2. 研究成果在學術期刊發表或申請專利等情形：

論文： 已發表 未發表之文稿 撰寫中 無

專利： 已獲得 申請中 無

技轉： 已技轉 洽談中 無

其他：（以 100 字為限）

在論文發表方面，累計相關國際會議論文發表五篇（其中兩篇與林大衛教授合作），已有三篇會議論文轉為期刊論文投稿，但過程未如人意，目前尚在評審中。

一項專利申請案已通過校內審核，一項剛立案。

3. 請依學術成就、技術創新、社會影響等方面，評估研究成果之學術或應用價值（簡要敘述成果所代表之意義、價值、影響或進一步發展之可能性）（以 500 字為限）

總結我們的技術成果，在於解決合作式通訊(分散式多輸出入系統 distributed MIMO)在搭配 Alamouti 編碼或是 BICM 的情況下之同步問題，以及高速移動下可能面臨的載波間干擾問題。我們提出一個可評估載波間干擾嚴重性並隨時調整的處理架構，有效降低了運算成本，確實為業界所需之實用性技術。我們也發展了兩套傳輸架構，兩者皆有極佳的同步誤差容忍度，在文獻中尚未見到有可和我們比肩的結果。我們認為，這項成果，對合作式多輸出入系統的實用化有很大的意義，將來也是業界可憑藉實現 4G 手機的武器。唯目前開發的接收機演算法仍具高複雜度，降低運算複雜度我們努力的方向。